15

Porous Silicon Sensors - from Single Layers to Multilayer Structures

J.E. Lugo, M. Ocampo, R. Doti and J. Faubert
Visual Psychophysics and perception laboratory School of Optometry
University of Montreal
Canada

1. Introduction

1.1 Origin and discovery

Silicon, one of the more common elements in nature, is defined as a metalloid, which corresponds to the number 14 in the Mendeleyev Periodic Table. It is heavier than Carbon (element number 6 in the periodic table and a key component in biochemistry), but both have chemical characteristics that are very close. Since human civilization began, volcanic stones containing this metalloid in the form of dioxide were used to create the first tools and weapons. Roman historian Plinio the Elder (23AD-79AD) mentioned the *Silex-Silicis* (silicon stones) in one of his works as very hard stones. These roman words are the *Latin* origin of the name Silicon (Tomkeieff, 1941).

J.J.Berzelius was credited for the discovery of this element in 1824 in Stockholm, Sweden, but Gay-Lussac and Thenard had already prepared impure amorphous silicon by 1811. After World War II, once the applied mechanical technology was ready to produce very pure silicon wafers (under the form of monolithic crystals) and succeeded to manage the problem of the surface impurities and contamination (Hull, 1999), the electronic industry jumped from the Germanium diodes to the Silicon integrated circuits and metal-oxide-semiconductor (MOS) microprocessors that helped man reach the Moon. In summary, it is safe to say that Silicon's role along our evolution extends from prehistoric times to the exploration of the Solar System.

In 1956 at the U.S. Bell Laboratories, Arthur Uhlir Jr. and Ingeborg Uhlir while trying a new technique for polishing Silicon crystalline wafers observed for the first time a red-green film formed on the wafer surface (Kilian et al, 2009). Since the discovery of its luminescence properties by Leigh Canham in 1990 (Kilian et al, 2009), researchers started to study the nonlinear optical, electric and mechanical properties of this nanostructure. This effort has permitted the fabrication of uniform porous layers with diameters as small as one nanometer, and permitting an enormous inner surface density.

2. How to prepare porous silicon (p-Si)

Several techniques exist to form this structure from a pure Silicon crystalline wafer. The most popular are: electrochemical etching, stain etching and photochemical etching. Here we introduce two versions of the etching process (Anglin, n.d).

2.1 Electrochemical etching

As shown in the figure 1, we have a Si wafer (single crystalline) with the top face in contact with a hydrofluoric acid solution and where an immersed platinum electrode is placed at certain distance from the wafer and parallel to it. In the bottom face of the wafer we find a flat metallic electrode that is in close electric contact. Between the two electrodes there is a controlled voltage supply with its negative pole connected to the platinum immersed electrode. A current is established from the anodic electrode (back of the wafer) and the catodic electrode (platinum immersed). Modulating four variables: the intensity and interval of application of this current, the HF solution concentration, and the concentration and type of dopant previously applied to the Si wafer (type-n, type-p, or highly doped: type-pp and type nn) it is then possible to control the porous size and p-Si layer geometric parameters, as well as the number of layers. Dopant refers to a different element atom that replaces a percentage of the Si atom inside the wafer and that is compatible with it in a crystallographic way, but that presents an electron in excess (type n) or an electron lack (type p). This introduces a number of properties that modify the material behavior when an electric field is applied, mainly the resistivity, that will influence the etching process performance. The electric current oxidizes the surface silicon atoms permitting a fluoride attack on them generating the pores. It is also possible to create multilayer structures by alternating different current densities. For instance, if we start making the first layer with a current density J_1 then the final porosity (and the refractive index) is going to be approximately determined by this current density. The electrochemical reaction time determines the thickness. By switching the current density to a different value J_2, something amazing happens, the reaction continues mostly at the crystalline silicon interface, leaving an almost intact first layer. Then the second layer will have a different refractive index and thickness (if we readjust the reaction time). Porosity can be measured by gravimetrical means. That is, the original crystalline silicon wafer is weighted first, then p-Si is formed and the wafer is weighted again, finally the p-Si layer is removed by adding KOH (Potassium hydroxide) and the wafer is weighted once more. With these three measurements is possible to determine the porosity. To measure the thickness, SEM (scanning electronic microscopy) techniques are normally used giving the best resolution and accuracy. Refractive index is usually determined by optical interference methods, where the refractive index can be estimated by taking adjacent maxima or minima from interference fringes coming from the p-Si sample.

Stain etching: In this procedure the power supply action is replaced by the chemical oxidant action of nitric acid. The reaction control is performed trough the addition of other additives. Results are less homogeneous than those of the first process described, but they still permit to have the material quality compatible with several applications.

3. Different types of p-Si sensors. Overview

Sensors allow our systems and devices to be in relation with the real events that we need to register or control. So, precision (same response to the same stimuli: repeatability) and accuracy (indicating magnitude value as close as possible to the real magnitude of the stimulus to be sensed: minimum absolute error spread) are two main requirements for any sensor when the industry selects its type or structure for market use. However, other properties will define the success of a new kind of sensor in the market. These are:

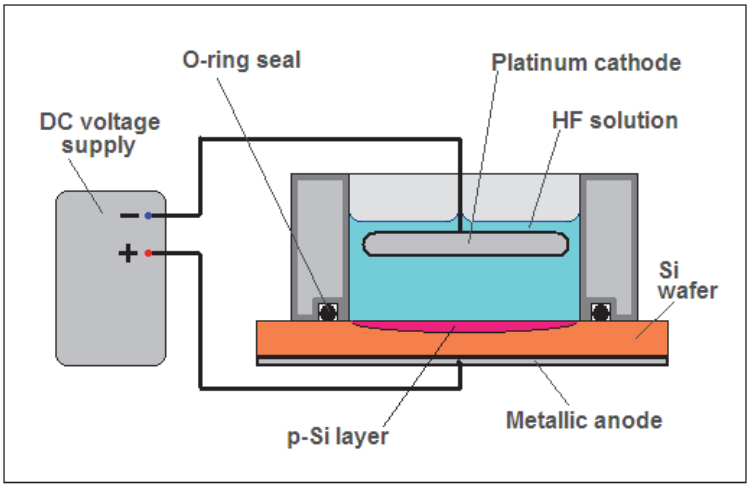

Fig. 1. Experimental setup for porous silicon fabrication.

technological compatibility with the existing devices, geometric dimension requirements, low noise insertion, ease of adjustment and setup, low power consumption, performance standardization (linear if possible), low thermal or aging characteristic drifts, robustness, reliability, low obsolescence, and very wide field of applications. P-Si is a material that accomplishes all of these requirements with enough margins to think that it will become increasingly popular in the short term.

For instance, integrated circuits (IC) are made of crystalline Silicon, which means it is fully compatible for associating a p-Si sensor to any electronic device. The electrochemical technology used to create a p-Si layer does not collide with the IC lithography. The geometric dimensions required to create this type of sensor are sufficiently small to be integrated in an IC. The homogeneity of the porous and its radius control (internal surface density control) as well as its layer stability is improving very fast. We can create a vast range of p-Si structures ranging from photonic crystals, a diffusive absorption electric material, a characterized geometry surface chemical reactor material, etc. The number of potential sensing applications is very large and is still growing daily (Angelucci et al, 1997).

In this section we present an overview of several types of p-Si sensors. Although not an exhaustive description, we cover a wide range of applications to illustrate the possibilities of putting the special characteristics of this material to work. We must consider that the p-Si application field is object of new developments practically everyday.

3.1 P-Si Biosensors: optical properties changes

Medical automated diagnostic, specific biological fluid concentration dynamics and molecular recognition are some of the expanding needs to be satisfied in the biomedical, veterinary and food industry. All of them could be achieved by this kind of sensors.

Research in this field was pushed by the discovery of the light emission capacity of the p-Si material (Cullis & Canham, 1991). The main consequence of this fact was considering the p-Si optical properties changes to detect target substances in function of the ability to trap molecules given by the boundary chemistry that occurs in the inner porous surface and its special characteristics (800 m^2 per gram).

3.1.1 Refractive index transduction

The mechanism referred to the absorption or diffusion of a complex molecule substance into the p-Si material could be complex and dependent on the geometry of the porous layer, the surface chemistry activity and the physical conditions present. We will try an intuitive simplified description of this type of detectors.

As shown in figure 2, a cell equipped with a transparent window contains a p-Si specimen which surface is in contact with a solution flow. The window is swiped by a special fiber optic tip linked to an interferometer. The fibers have two functions: a) providing white light from a special lamp, and b) picking up the reflected light to send it into the interferometer

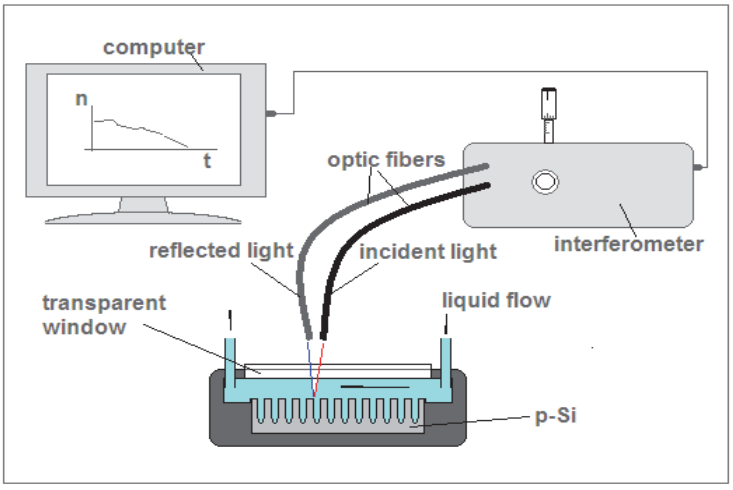

Fig. 2. Scheme showing the refractive index transduction.

that will let to obtain the System Reflectance Spectrum. This specific online info will give us, by means of a computerized algorithm, the evolution in time of the p-Si refraction index **n.** In this case the change in the reflectivity spectrum is a function of the DNA hybridization between an immobilized reference DNA (molecules attached to the porous surface) and a target DNA in solution (Jane et al, 2009). This event modifies the reflected light spectra in a way that is suitable of being quantified, thus configuring a bio-sensor.

3.2 One-dimensional photonic crystals (1 D)

When the specimen structure corresponds to a one-plane multi layer p-Si crystal we are in presence of a 1D photonic crystal (see figure 3). This geometry offers better reflectance spectra (without side lobes) if compared with a mono-layer structure. Combining the layers dimensions (layer thickness, porous density and radius, number of layers, etc.) we can tune the different layer's refraction index **n,** and according to the global geometry we can tune the average refraction index, $\mathbf{n_m}$ for the specimen. This kind of geometry permits create Bragg reflectors and Micro cavities (Lee & Fauchet, 2009**)** which reflectivity shows defined functional dependence when liquid solutions or gases are in contact with the p-Si specimen.

Once again the set up configuration is similar to the figure showing the fiber optic interferometer. The figure below refers to the characteristic reflectance spectra for these two

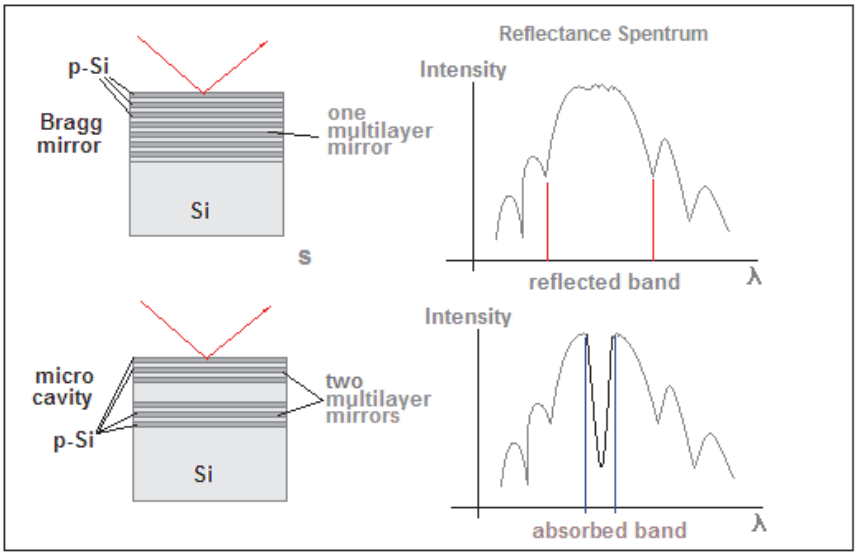

Fig. 3. Scheme showing two different one-dimensional photonic arrays of sensors.

types of photonic crystals. The difference between the incident light spectrum and the Reflectance Spectrum is the energy absorbed (refracted light) by the crystal bulk (Jalkanen et al, 2010). Finally, we would like to mention that this reflection mechanism shows in addition another important characteristics as the polarization of the reflected light (TE or TM) where the Transversal Electric or Transversal Magnetic components of the traveling electromagnetic wave (in our case the incident light) are discriminated by the photonic crystal reflection mechanism.

3.2.1 Reflectance spectrum shifting mechanism

The presence or absence of a target molecule in the liquid solution can be determined as follows:

First, we obtain the reflected light spectrum with the device filled only with the solution solvent: for instance: water (this is equivalent to zeroing our instrument). It will be the reference reflectance spectrum.

In the next step we introduce into the liquid flow the substance containing the target molecule, while computing the modified reflected light spectrum.

The modified spectra will be shifted (Baratto et al, 2002) in the light wavelength domain with respect to the reference spectrum depending on:

- whether or not the solution is capable to go into the channels of p-Si, or it's rejected
- the surface chemistry creates bonds that attach or not the target molecules against the channels walls (this can be controlled by a previous surface oxidation)
- the type of bond attaching the molecules to the surface: ionic, covalent, etc.

-the refraction index of the substances involved, that is function of their solution concentration and that depending on the device geometry will result in a global refraction index valid for the device considered as an unit. In the figure 4, we present, as an example, the detection two types of molecules together.

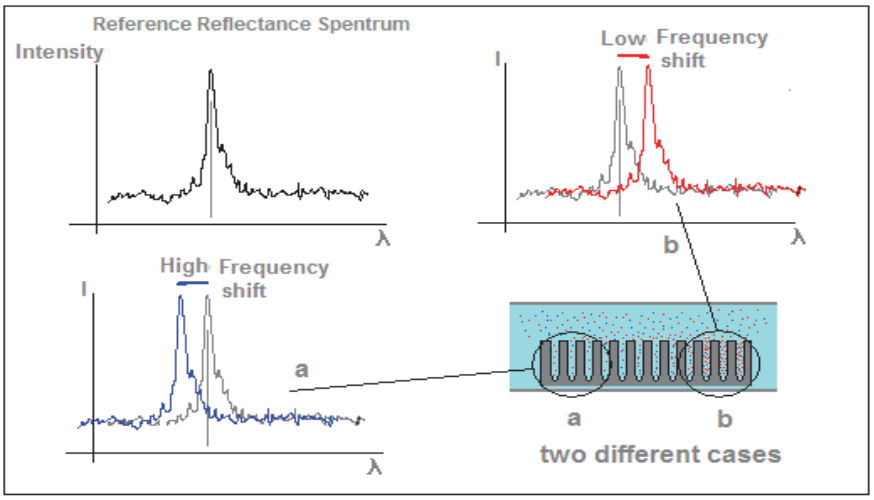

Fig. 4. Optical detection examples for two different types of molecules.

In the case a) the blue molecules are kept outside of the p-Si structure due to the surface chemistry bonds and reducing their presence inside de structure channels. The resulting lowered density of blue molecules inside the channels reduces the global refraction index, as well. This change in the device refraction index shifts the reflected spectrum towards the higher frequencies (shorter wave length). This effect is called blue shifting.
In the case b) instead, the red molecules are induced to get into the channels increasing their density. As result, this time the global refraction index is increased and the reflected spectrum will be shifted toward the lower frequencies (longer wavelength). This is called red shifting.
The reader must have into account that in the above discussion both types of situation were introduced together in order to improve the comprehension of this mechanism. In real life, and due to the complexity of the conditions and detection thresholds to achieve, only one type of target molecule is present in the experiment. Furthermore, the whole device is conceived and designed to increase its detection capabilities in function of the specific target molecule.

3.2.2 Photoluminescence transduction

This refers to the emission of photons (called secondary photons) when the p-Si specimen is excited by a light beam (primary photons). This phenomenon was verified at room temperature around twenty years ago. The principle for this type of biosensors is based in the photoluminescence quenching (PQ) that takes place when the specimen is in contact with a target substance. Applications cover from organic solvents, biological waste, and molecular recognition (Di francia et al, 2005). This type of sensors is delicate and sensible to interfacial charging that can affect their performance. The experimental set up is similar to that shown in the figure 4. The comparison between the returned light spectrum, whether is present or not the target substance in contact with the p-Si, is the parameter that lets scale the sensor. We could say that this is a Frequency Converter mechanism. From the incident energy, normally a short wavelength close to, one part is reflected and from the absorbed

portion a fraction is origin of a longer wavelength light emission: normally red. This new component is not present in the incident spectrum, but it appears in the reflectance spectrum as shown in figure 5.

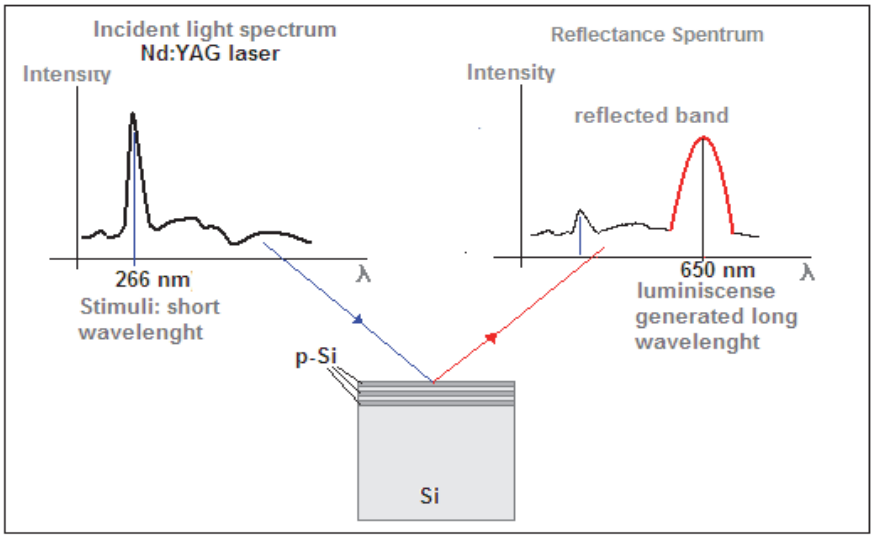

Fig. 5. Scheme for the photoluminescence transduction.

3.2.3 Capacitive transduction

The physic property by which it is possible to storage electric charge between two conductive materials, or the equivalent that is to storage electrostatic energy, is called capacity. The simplest geometry for configuring a capacitor, device which has this property, is to have two flat metallic surfaces separated by a dielectric material (typically an isolator). The relationship between the superficial electric charge density accumulated in both metallic planes and the external electric field applied to a planar p-Si specimen is known as the Dielectric Constant. When considering a particular geometry, this constant lets measure the Capacitance of the whole device. The arrangement fundamentals are shown in the figure 6.
The capture of target substances molecules in the surface of the specimen varies the Surface Charge Density, thus the Capacity of the whole device. This effect lets to scale the system as a biosensor by correlating the device electric capacity to the presence and solution density of the target molecule. The complete electric model for the sensor is composed by a capacitance associated to a parallel and a serial conductance (representing relaxation constants of the material according to the working frequency) that make necessary to assess the impedance spectroscopy (Baratto et al, 2001) to determine the particular frequency at which we have the maximum gas sensitivity.

3.2.4 Conductance transduction

The relationship between the current in Amperes circulating trough a piece of a given resistive material and the value of the potential difference in Volts applied to originate that current is defined as the conductance of that resistive piece. This could be interpreted as the

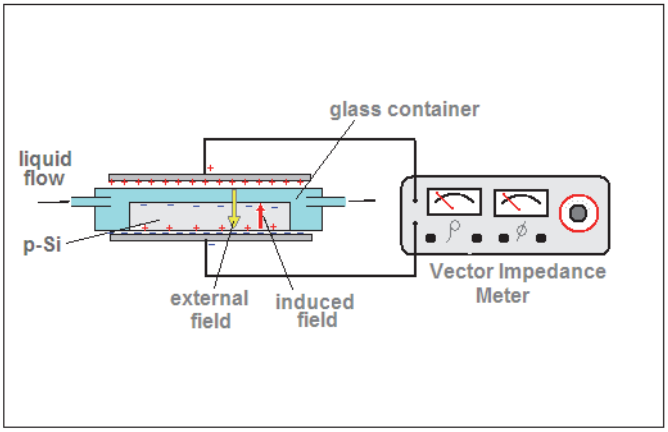

Fig. 6. Scheme showing the capacitive transduction mechanism.

facility that a material offers to let a current circulate trough it per unit of Volt applied. The conductance unit is the Siemens (S).

The phenomenon is related to divers mechanisms by which the electrons contained in a, for instance, crystalline structure are enable to circulate trough that structure. These mechanisms could cover from a simple action of the external electric field applied, to complex electron interactions between specific energy levels inside the atoms.

The existence of a dominant geometrical characteristic such as the inner porous, and its inherent enormous surface density, makes p-Si very susceptible for conductance dependence on the environmental conditions. And from the beginning several types of sensors were conceived on this basis to detect: relative humidity, gases, alcohol, and organic vapors in general (Choi et al, 2009).

With this objective, p-Si geometric parameters have been tuned to maximize conductance detection of different target molecules, presenting each resulting device a big discrimination between targets, even if the response has a systematic fading in the time domain. In figure 7 you can see the specimen with two gold plated surface terminals that let connect it to a DC source by means of an ammeter and a resistor of 1 kilo ohm. A voltmeter reads the resistor voltage drop: V_R. This is the output signal of the system when the vapor or gas flow is in contact with the specimen. The graphic represents the normalized value of V_R in function of time, where '**m**' (blue) represents the output for *Methanol*, ' **i** ' (green) for *Isopropyl Alcohol*, and '**a**' for *Acetone* (Choi et al, 2009) .

As you can see the response of the sensor is specific for each molecule. But the output is not constant along the time because of the vapor penetration in the porous. Exist a delay (several minutes) after the flow is enabled (valve open) to get the maximum output voltage level. We observe an override of the output signal (peak) after the valve is closed (flux off). In addition exist a recovery time (not indicated) needed by the sensor for returning to the initial sensibility. Another aspect to consider is the **t**hermal drift (that can be manage by controlling the environmental temperature), and the aging effect that reduces sensibility in few month of use. Engineers have to overcome all these difficulties and unexpected behaviors to produce a reliable sensor, even if its performance is based on a simple and stable principle. This situation extends, and somehow in a more complex way, to all the other types of p-Si sensors discussed.

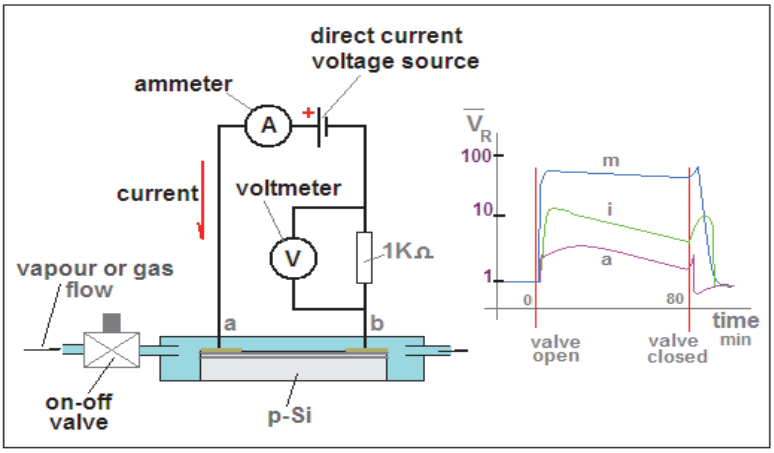

Fig. 7. Conductance transduction scheme.

4. How to make p-Si selective to different chemical and biological compounds in three specific examples

P-Si possesses a large internal surface area ranges from 90 to 783 m^2/cm^3 (Chan et al 2001) which provides numerous sites for many potential species to attach. It has been proposed as the substrate material for sensing applications because it can readily be integrated with silicon technology. Different methods and mechanisms were used for p-Si formation, the bulk of which can be classified as electrochemical (Chan et al, 2001; Lugo et al, 2007; Archer et al, 2005), photoelectrochemical and 'stain etching' methods that do not require light or electrical bias. The most common method used is the anodisation under galvanostatic conditions. Both phosphorous (n-type) and boron (p-type) doped silicon can be electrochemically etched in aqueous and/or organic electrolyte solutions containing HF to yield a range of nano- to micro-scale structures by simply selecting the appropriate dopant concentration of the Si substrate and/or adjusting the anodisation conditions (Kilian et al, 2009). According to its pore sizes, p-Si can be classified as macroporous (pore diameter $d > 50$ nm), mesoporous ($2 \text{ nm} < d < 50$ nm) and microporous ($d < 2$ nm). Diameter of DNA molecules is approximately 5 angstroms. Therefore, the p-Si pores size must be in the order of nanometers to allow infiltration of the biomolecules to be useful to optical biosensing. This is the main reason to focuses on mesoporous silicon to accommodate biological species. The sensitivity of the surface to chemical species has been demonstrated by exposing porous silicon layers to different compounds, such as vapors, molecules with different dipole moments, DNA, small viruses and bacteria (Ben-Chorin et al, 1994; Schechter et al, 1995; Chan et al, 2001; Archer & Fauchet, 2001). In the development of a sensor, selectivity is a very important issue because the sensor must be able to distinguish the element being sensed. For biosensors the bioselective element is usually immobilized on some sort of support (Chan et al, 2001), p-Si in this case. The sensor is then exposed to the species being sensed and the output signal is detected. To obtain a high quality sensor the p-Si layers must be made by choosing the appropriate anodization conditions. DNA biosensors based on nucleic acid recognition processes are rapidly being developed with the goal of rapid and

inexpensive testing of genetic and infectious diseases. The use of DNA recognition layers represents an exciting development in analytical chemistry (McGown et al, 1995). Electrochemical biosensors have received a great deal of attention due to their high sensitivity and rapid speed of detection. In addition, electrochemical techniques are ideally suited to miniaturization and have the potential to simplify nucleic acid analysis using low-cost electronics (Yan et al, 2001). Nowadays, they are being used in many reports for detecting the DNA hybridization event, due to their high sensitivity, small dimensions, low cost, and compatibility with microfabrication technology (Yan et al, 2001; Kara et al, 2002; Wang, 1999; Erdem et al, 1999; Marraza et al, 2000; Maruyama et al, 2001; Shi et al, 2004).

4.1 First example: an electrical sensor

To prepare the porous silicon layers, Archer et al (Archer et al, 2005) use N,N dimelthylformamide (DMF) under galvanostatic conditions of p-type silicon (resistivity ~ 10-20 Ohm-cm) with a current density of 4 mA/cm^2. The electrolyte could be a 4 wt% hydrofluoric acid (49 wt%) in N, N dimethylformamide (DMF). The use of a mild oxidizer, such as DMF, results in a straight and smooth pore walls with pore diameter in the micrometer range (Archer et al, 2005). These conditions were selected to increase the pore diameter and to enhance the sensitivity to changes in the space charge region. The porous layers were etched for 70 min resulting in 20 microns thick layers. To stabilize the p-Si device a thin layer of surface oxide is required for proper operation. The layers were thus chemically oxidized by immersion in 30 wt.% of hydrogen peroxide (H_2O_2) for a period of 48 h at room temperature (22 Celsius degrees). Although the oxide layer produced by this oxidation technique is very thin. The oxide is hydrophilic enough to allow the infiltration of water soluble molecules without the need of a thicker thermally grown oxide. After oxidation the porous layers were rinsed with deionized water and ethanol and dried under a stream of nitrogen. The oxide on the backside of the crystalline silicon substrate was stripped with a 15% HF solution (7:1, water: 49 wt % HF) prior to the contact placement. The wafers were cleaved into sections of 4 × 7 mm and two coplanar electrical contacts were placed 700 μm apart on the crystalline silicon substrate. In this approach, the p-Si surface is completely exposed to the sensing molecules and no metal contacts are made to it, avoiding the introduction of foreign materials into the porous matrix (Archer et al , 2005). In order to avoid any of the solvents tested from reaching the backside contacts, the sensors were fixed on a glass slide, which ensures a horizontal surface for a uniform distribution of the solvent on the porous layer and protects the backside of the device.

4.2 Second example: an optical sensor

Precise control of the nanocrystalline size distribution is extremely difficult; therefore, an alternative method is required to reduce the luminescence bandwidth (typical fwhm ~ 150 nm). Selena Chan et al. (Chan et al, 2001) developed a device nanostructure, which solves this problem. It consists of a microcavity resonator composed of various porous silicon layers, prepared electrochemically (Chan et al 2001). By confining the luminescence generated in the central layer of the microcavity by two Bragg reflectors, the photoluminescence spectrum is composed of multiple sharp and narrow peaks with fwhm values = 3 nm. Upon a refractive index change, the photoluminescent spikes shift, thereby generating a large, detectable differential signal. Selena Chan (Chan et al, 2001) presented an optical approach to detecting Gram-(-) bacteria based on the principles of light interference

across multilayers of varying refractive indices. By properly functionalizing the inner surface of a porous silicon layer with highly selective receptor molecules aimed at specific targets, multisensor arrays can be designed to quickly determine the presence of certain pathogens. The porous silicon surface was treated with a 3-glycidoxypropyltrimethoxy silane subsequent exposure of this epoxide-terminated surface to an aqueous solution of tetratryptophan *ter*-cyclo pentane (TWTPC) at 6%, dimethyl sulfoxide (DMSO) provide a surface functionalized with the lipid A-bonding receptor. However were found that the procedure with purified diphosphoryl lipid A do not produce a functional devices (Chan et al, 2001). This conduces to an assumption that all four groups of the tetratryptophan receptor react with the functionalized porous silicon surface, thus blocking access to the binding face of the receptor molecule. If this were indeed the case, we hypothesized that exposure of the epoxide-terminated surface to a mixture of TWTCP and a "blocking" amine would allow for the generation of a functional sensor. Using glycine methyl ester as the blocking amine and examining the response of the sensor to purified lipid A, they found that the optimal ratio of receptor to blocker molecules was 1:10 TWTCP:glycine methyl ester (Chan et al, 2001). In this case, incubation of the sensor with a solution of lipid A produces an 8 nm redshift in the photoluminescence peak wavelength. When a 100% solution of TWTCP or a 100% solution of glycine methyl ester is immobilized in the porous matrix, no shifting of the luminescence peaks is detected after exposure to lipid A.
To determine the ability of this sensor to differentiate between two classes of bacteria, independent overnight cultures of Gram- (-) bacteria *(Escherichia coli)* and Gram-(+) bacteria *(Bacillus subtilis*) were grown up, centrifuged, and then individually lysed following resuspension in phosphate buffer solution (PBS, pH 7.4). Upon exposure of the lysed Gram-(-) cells to the immobilized TWTCP biochip, a 4 nm photoluminescence red-shift was detected. However, when the microcavity sensor was exposed to a solution of lysed Gram-(+) bacteria, no shifting of the luminescence peaks was observed. We attribute the large shift to the recognition and binding of the TWTCP receptor with the lipid A present in the bacterial cell wall. Analogous results were obtained with several other species of Gram-(+) and Gram-(-) bacteria. These results demonstrate the ability of a p-Si biosensor to distinguish between Gram-(-) and Gram-(+) bacteria. Clear modulation of the photoluminescence spectra from microcavity device structures illustrates their application as biosensors that can translate the recognition of lipid A present in bacterial cell walls into an optical signal. The remarkable features of these silicon sensors (integratable, high surface-to-volume ratio, robust, inexpensive, small, ease of use) should allow arrays to be constructed to simultaneously identify a variety of analytes by simply functionalizing the surface with arrays of specific, high affinity receptor molecules.

4.3 Third example: an electrochemical sensor

Lugo et al (Lugo et al, 2007) describes the use of p-Si layers to transduce hybridization of DNA into a chemical oxidation of guanine by $Ru(bpy)_3^{2+}$, the reduced form of which is then detected electrochemically. Nucleic acid modified p-Si electrodes were used in combination of voltammetry for the detection of DNA. $Ru(bpy)_3^{2+}$ were used as electrochemical hybridization indicator for DNA detection. It has been shown (Johnston et al, 1994; Johnston et al, 1995; Johnston & Thorp, 1996; Napier et al, 1997) that Ruthenium $Ru(bpy)_3^{2+}$ is a better indicator for quantitative determination of short gene sequence such as the ones used in those experiments. The DNA probe sequence, immobilized at the electrodes, was

engineered in a similar way as in (Napier et al, 1997) to decrease the oxidation of the probe DNA with $Ru(bpy)_3^{2+}$. Such a sequence does not contain the guanine but inosine. Inosine is three orders of magnitude less reactive than guanosine and still recognizes cytidine which is very important for sensing all four bases in the DNA target sequence.

In another experiment (Lugo et al, 2007) p-Si samples were prepared from p+-type, boron doped silicon wafers with a resistivity of 0.008-0.012 Ohm.cm by standard anodization (electrolyte: 15% of HF) at a current density of 30 $mA.cm^{-2}$. The porosity was measured by the gravimetrical method given a porosity of approximately 62%. The pore size was estimated by TEM and ranged from 50 nm-75 nm in diameter. These diameters are large enough to allow the sensing molecules to penetrate and attach. For DNA, the diameter of the nucleotides is approximately 5Å, which is small enough to fit into the porous matrix. Stabilization of p-Si is necessary to passivate its surface and this was done by thermal oxidation. Thermal oxidation of p-Si requires several precautions and high temperatures (>700ºC). Covering the whole internal surface with a thin SiO_2 layer stabilizes the structure, permits water penetration into the pores, and facilitates probe and target penetration (Archer & Fauchet, 2007). All p-Si samples were thermally oxidized in oxygen ambient at 900ºC for 10 minutes.

Measurement set up used for these experiments is an electrochemical instrumentation that includes a BAS 100B/W Electrochemical Analyzer. A BAS VC-2 voltammetry cell (model MF-1065) was used for the electrochemical experiments. It is well suited to small sizes and has a special micro-cell for volumes as small as 50 microliters. The micro-cell, which includes the working electrode, separates a small volume containing the sample from a bulk solution containing the reference and auxiliary electrode with a salt bridge. A platinum wire serves as auxiliary electrode and the modified p-Si samples function as working electrodes. It is important to mention that p-Si, especially oxidized p-Si, is not conducting and it is in fact the p+ doped silicon that is conducting the electrical current. The top area of the exposed p-Si samples was 0.8 cm^2 and all lateral areas were insulated with a commercial epoxy resin (see figure1). The epoxy resin was deposited very carefully and dried for one hour. The samples were attached to the electrochemical system as shown in figure 1. Potentials were measured relative to an aqueous, saturated Ag/AgCl double junction (reference electrode). The voltammetry experiments were carried out at different scan rates in an electrochemical buffer solution composed by 50 mM sodium phosphate (pH 7) with 0.7 M NaCl. A schematic representation of the electrochemical measurement set up and the electrode arrangement is shown in figure 8.

4.3.1 DNA electrochemical detection procedure steps: p-Si, silanization, probe immobilization, hybridization, and voltammetric detection

p-Si Silanization. Several methods maybe employed to bind DNA to different supports (Archer & Fauchet, 2007). One method commonly used for binding DNA involves silanization of an oxidized surface. The function of silane coupling agents is to provide stable bond between two non-bonding surfaces: for example, an inorganic surface to an organic molecule. 3-glycidoxypropyltrimethoxysilane was used to silanize the oxidized p-Si. A 5% aqueous solution of silane was prepared (pH 4.0). This converts silane into a reactive silanol through hydrolysis. The p-Si samples were then immersed into the continuosly stirred solution and left overnight. 3-glycidoxypropyltrimethoxysilane is hydrolyzed to a reactive silanol by using double distilled water (pH 4). Porous silicon samples were then submerged into silanol solution for approximately 17 hours. Constant stirring of the solution was necessary to continuously mix the solution.

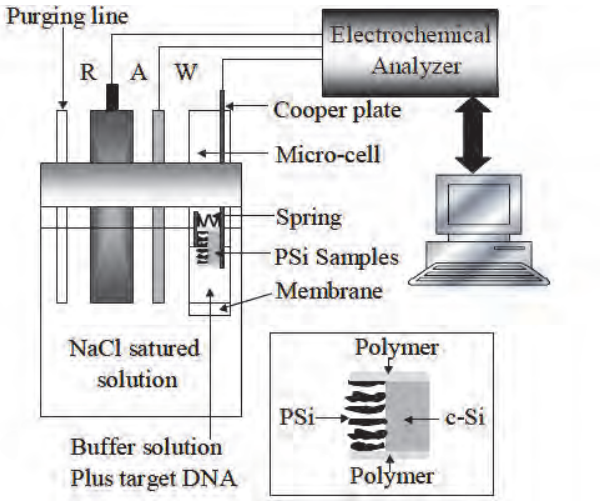

Fig. 8. Measurement system: the p-Si electrode is used as working electrode. A platinum wire is the auxiliary electrode and Ag/AgCl the reference electrode. Inset: cross section showing the different parts of the working electrode.

Probe immobilization After successful silanization, DNA is immobilized onto the surface of p-Si through diffusion. Aqueous solutions of DNA containing 150 microliters of DNA (50 microM) were carefully placed directly above de p-Si layer. The DNA molecules covalently bond to the silanized surface, where they become immobilized. The samples were then placed in a steam container where they were heated in an oven at 37ºC for approximately 20 hours. The DNA attached samples then should be rinsed in double distilled water and dried with nitrogen.

Hybridization. The DNA attached to p-Si was exposed to its complementary strand DNA (target), the mismatch sequence (mismatch probe) and itself (probe). Binding was allowed to proceed for 1 hour at room temperature into hybridization buffer containing 1 M NaCl, 10-20 mM sodium cacodylate, 0.5 mM EDTA, 150 mM KCl and 5 mM $MgCl_2$. Throughout the steps, binding is confirmed using Fourier Transform Infrared Spectroscopy.

Voltammetric detection. Cyclic voltammetry (CV) was carried out having the DNA modified, p-Si electrode as working electrode, an Ag/AgCl as the reference electrode, and platinum wire as the counter electrode. 6 microliters of (0.1microM) was poured into 150 microliters of electrochemical buffer solution. After allowing the solution to diffuse into the samples for 15 minutes, CV was performed. Solutions were deoxygenated via purging with nitrogen for 10 minutes prior to measurements.

p-Si DNA-electrodes and $Ru(bpy)_{32+}$ were used for specific gene detection. $Ru(bpy)_{32+}$ exhibits a reversible redox couple at 1.05 V and oxidizes guanine in DNA at high salt concentration (Chan et al, 2001) according to:

$$Ru(bpy)_3^{2+} \rightarrow Ru(bpy)_3^{3+} + e^- \quad (1)$$

$$Ru(bpy)_3^{3+} + DNA \rightarrow DNA_{Ox} + Ru(bpy)_3^{2+} \quad (2)$$

where DNA_{ox} is a DNA molecule in which guanine has been oxidized by $Ru(bpy)_3^{3+}$. If the DNA probe contains guanine then $Ru(bpy)_3^{3+}$ will oxidize guanine in DNA, even without the presence of the target DNA. In order to prevent that the DNA probe reacts with $Ru(bpy)_3^{2+}$ the guanine has been replaced for another less reactive nucleotide. Some previous results show that the addition of an oligonucleotide that does not contain guanine produces a small enhancement in the oxidation current (Napier et al, 1997). Those results have shown that the inosine 5′-monophosphate is 3 orders of magnitude less electrochemically reactive than guanosine 5′-monophosphate and still recognizes cytidine (Napier et al, 1997). This fact is very important if we want to recognize all four bases in the target sequence. Nevertheless there is a drawback that can have consequences on the hybridization efficiency. Since the deaminated hypoxanthine in the ionosine can only form two of the three hydrogen bonds in a Watson-Crick base pair, it may be desirable to use a guanine derivative that is redox-inert but capable of forming all three hydrogen bonds. However some studies have shown (Napier et al, 1997) that the specificity afforded by inosine substitution was sufficient but they propose 7- deazaguanine as alternative. For this reason the DNA probe sequence does not contain the guanine base but the target does. Figure 2 (top) shows the CV obtained in solution for the hybrid DNA (probe-target) at different scan rates (target DNA concentration of 0.5×10^{-10}M). Figure 2 (bottom) shows that the anodic current of $Ru(bpy)_3^{2+}$ is linearly proportional to the scan rate. This result is congruent with a process that is controlled by adsorption. Figure 3 (top) shows the CV (scan rate of 50 $mV.s^{-1}$) of varied concentrations of target DNA (probe-target sequence, curves 2 to 5) and different targets (probe-mismatch target sequence, curve 1 and probe-probe sequence, curve 6). In curve 1, the mismatch target sequence contains two more pairs of base G than the target sequence and that is why the current in this case is bigger than the current obtained in the probe-target sequence cases (curves 2 to 5) or the probe-probe sequence (curve 6). Moreover in curve 6 the current intensity decreases as a consequence of the absent of the base G in the probe. Nevertheless a significant increase in current was observed for curves 2 to 5 where the target DNA undergoes hybridization to the complementary DNA. This current increase suggests that the hybridization was successful and that the electron transfer from the guanines of the hybridized strand to $Ru(bpy)_3^{2+}$ is responsible for the increase in the current. If we compare curves 1, 2 and 6 (same DNA concentration but different target sequence) we observe that the sensor responds differently to each target and therefore a good selectivity is achieved. Figure 3 (bottom) shows the anodic peak currents of $Ru(bpy)_3^{2+}$ at four different concentrations (curves 2 to 5). The peaks are linearly related to the concentration of the target DNA sequence between 0.5×10^{-10} and 500×10^{-10}M. The detection limit of this approach was 5×10^{-11}M. The sensitivity achieved in this work is similar to the one obtained in reference (Jalkanen et al, 2010), where a sensitivity of $9.0\text{x}10^{-11}$M was reported for a sensor that uses gold substrates instead. In summary this results clearly show that the electrochemical p-Si sensor shown here has a good selectivity and sensitivity to the target compound, two very important characteristics that a sensor ought to have.

5. Future optical sensors

Recently our group has studied the Negative refraction phenomenon in p-Si photonic crystals (Lugo et al, 2009; Lugo et al, 2011). Negative refraction refers that it is possible to bend light to the wrong direction of the normal at some interface between two materials. Let α be the incident angle of light. According to Snell's law, light impinging from air to a

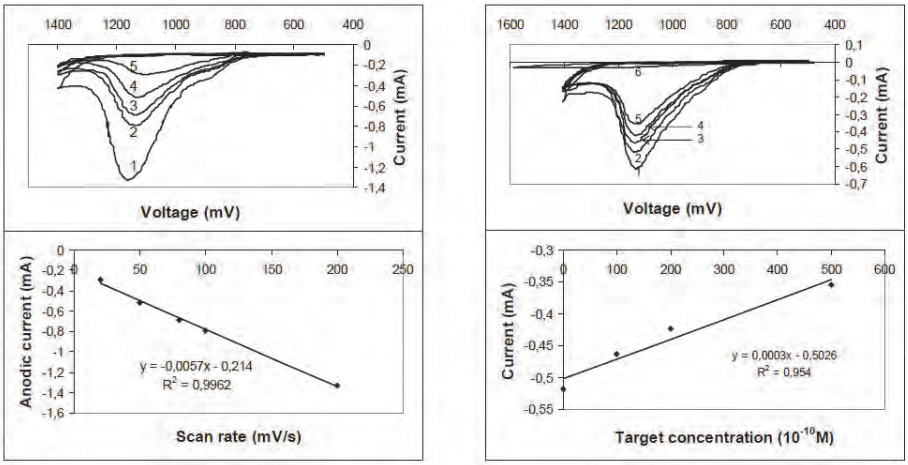

Fig. 9. (Left column, top) Cyclic voltammograms of the probe-target DNA sequence in 0.1 μM $Ru(bpy)_3^{2+}$ solution at different scan rates (mV.s-1): (1) 20; (2) 50; (3) 80; (4) 100; (5) 200. (Left column, bottom) The anodic current changes with the scan rate. The target concentration was 0.5×10-10M. (Right column, top) Cycled voltammograms of different concentrations of target DNA: (2) 0.5×10-10M, (3) 100×10-10M, (4) 200×10-10M, (5) 500×10-10M. Curve 1 shows the CV for the probe-mismatch target DNA sequence (0.5×10-10M) and curve 6 for the probe DNA sequence (0.5×10-10M). (Right column, bottom) The anodic current changes with the concentration of the target DNA. In all cases we have used 0.1 μM of $Ru(bpy)_3^{2+}$.

different material with bigger refractive index (like in figure 10) should cross the interface and continue traveling in the other side of the normal and actually bending towards the normal (the normal direction in this case is the line from where the angle alpha is measured). However in a one-dimensional photonic crystal that consists of a series of layers (80 in this case) "a" and "b" with indices of refraction n_a and n_b, it is possible to bend the light to the same side of the normal once the light crosses the interface (angle β'). This particular condition is found close to the bandgap edges corresponding to low energy or frequency edges of the second and fourth photonic bands once the indices of refraction and thickness have been properly tailored.

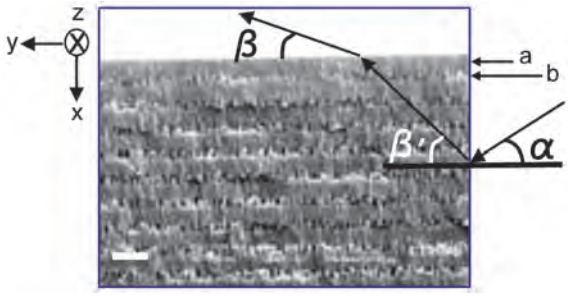

Fig. 10. One-dimensional photonic crystal picture. Showing the light path that a negative refraction beam follows.

Experimentally, the way to observe the negative refraction beam is described in figure 11. The sample (Component 6) with the pinhole (Component 4) was illuminated by a broad band source (Component 1) and to obtain the desired monochromatic light we have used two band-pass filters (Component 3) at 633 nm and 1350 nm (both have a 10 nm bandwidth). The TE or TM polarization was selected by using two linear polarizers (Component 2), and the negative refractive transmitted light was captured by two CCD cameras, one for the visible range and a second for the infrared region coupled with a singlet lens (Component 9) placed at 8 mm from the sample. The sample and the camera were mounted on linear and rotary mechanical stages. The XYZ linear stages had a resolution of 1 micron and the rotary stages had a resolution of 2.5 arc minutes. The TE or

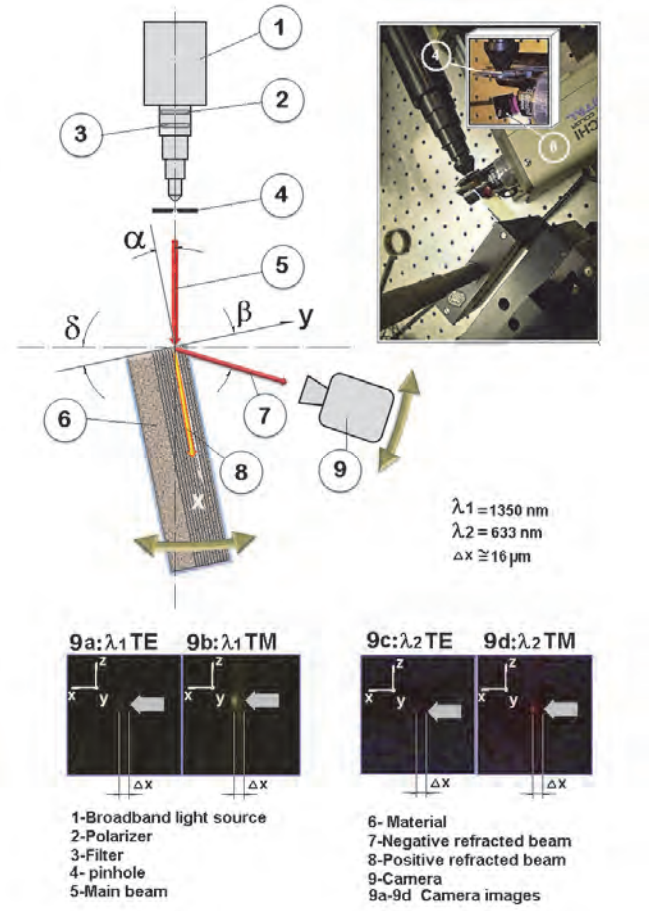

Fig. 11. A cartoon of the experimental setup (with the nine components) for the negative refraction observation and a picture of the real experimental setup. Both the sample and the camera are placed in translational and rotational stages. A broadband source along with bandpass filters and linear polarizers were used to explore the infrared and visible negative refraction bands. Captured images for the different conditions are shown in 9a-9d.

TM Polarized monochromatic light beam (Component 5) illuminated the sample at an angle of 25 degrees through a 1 mm pinhole placed at 3 mm from the sample. The beam was focused in the x-direction interface in a way that light never hit the y-direction interface. This was performed very carefully by scanning the focused light beam from the crystalline silicon substrate towards the y-direction interface. The cameras were centered at 25 degrees (angle β') but their positions were compensated to account for the positive refraction that the negative refraction beam (Component 7) suffers at the exit of the y-direction interface (angle β'). This was done by using Snell's law and an effective refractive index value of 1.6 for the multilayer structure. Once everything was in place we scanned the sample on the z-direction (see component 9) and when a spot image was captured we measured the distance from the x-direction interface to the image (Δx was corrected due to the sample rotation) by using the micrometer screw of the linear stage. This was possible because our imaging system was capable to give us enough resolution to mark on a screen the x-direction interface and the spot image. The components 9a-9d shows four images corresponding to 1350 nm and 633 nm (TE and TM polarizations). The spots are located at a distance of approximately Δx = 16 microns from the interface (x-direction) which agreed with our numerical simulations.

Now, how we can implement a sensor based on this wonderful property? One answer is that we can introduce a chemical compound or a biological agent that would increase the refractive index of each layer. As a consequence the negative refraction condition (at certain angle of incidence) would be altered and the output angle β would not be the same. Since, this angular difference is proportional to the increment on the refractive indices and this refractive index increment is proportional to compound concentration, therefore compound concentration would be proportional to the angular difference. We performed full-wave simulations for TE polarization light considering the experimental thickness and refractive indices we found in references (Lugo et al, 2009; Lugo et al, 2011). The optical losses were neglected and we simulated 80 periods. The first results are shown in Figure 12 (Top). We can observe that for visible light (633 nm) with an incidence angle of 15 degrees there are three beams propagating inside the multilayer. The one that travels to the top of the multilayer is the negative refraction beam, the one that travels parallel to the multilayers is known as a waveguide mode and the last one that goes downwards is the positive refraction beam. What happens if we increase the refractive indices of the layers by 0.1 %. The answer is displayed in figure 12 (Bottom). Where we can see that beam propagation directions drastically change. The negative refraction angular change is of the order of 30 degrees, which shows that this sensor might be very sensitive when working with this beam and we believed can achieve a sensitivity similar to the one found in (Saarinen et al, 2005). The waveguide mode can be used for sensing applications as well because the beam intensity decreases and shifts spatially. Although the change is not dramatic as in the precedent case, it is still useful for sensing higher compound concentrations, for instance. Finally the positive refraction angular change is of the order of 12 degrees and this beam can be used in a similar way as the waveguide mode.

Final remarks:

Porous silicon has been demonstrated as a suitable host for different sensing applications. Porous silicon has been shown to be an ideal sensor material for various compounds and the variety of sensing applications ranges from alcohols to bacteria. On the other hand p-Si has

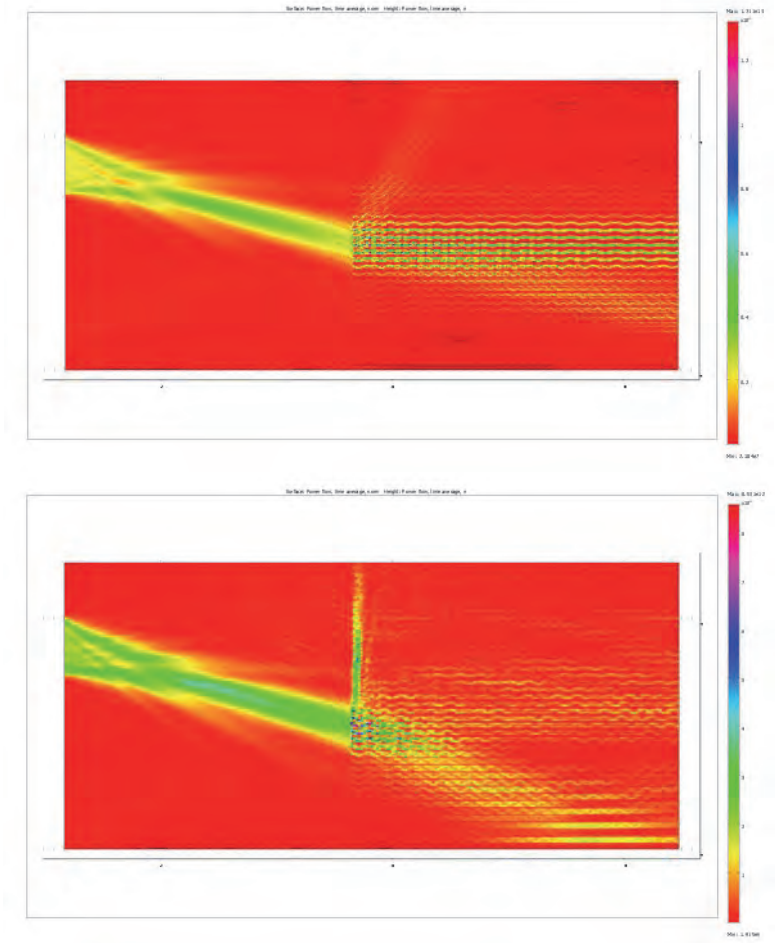

Fig. 12. (Top) Finite element simulation of a one-dimensional photonic crystal consisting of 80 layers with alternated refractive indices. Light of 633 nm impinges at an angle of 15 degrees and then splits up in three beams. The negative refraction beams goes towards the top of the structure. The waveguide mode beam travels parallel to the surface of the layers. The positive refraction beam goes downwards. (Bottom) After increasing 0.1% the refractive indices in the structure the negative refraction beam changes drastically its direction. The waveguide mode and the positive refraction beam change their direction as well but it is less pronounced than in the negative refraction case.

originated several proof-of-principle studies such as electrochemical, electrical and optical transducers. The latter have been intensively studied and are based on photoluminescence effects, reflective interference, or photonic resonance. Porous silicon sensors are promising platforms for pharmaceutical applications because it is highly absorbed by our bodies and also has low toxicity properties. Porous silicon technology allows us to control pore size from a few nanometers to several hundreds of nanometers in diameter. Porous silicon surface can be

modified by chemical methods with different compounds ranging from organic to biological molecules (proteins, bacteria, peptides, antibodies, etc.). The impressive optical properties of this material may provide us with a wonderful tool for in vivo sensing or therapeutics. For instance, its luminescence and the unique reflectivity spectra of multilayers are two features that allow p-Si to exhibit a signal that is modified in a predictable way when exposed to environmental changes. Another important property is that p-Si may be easily integrated into standard silicon microelectronics techniques. This integration would be beneficial for medical applications because we would be able to create more sophisticated active devices. However, there are several challenges that p-Si sensing technology has to overcome before having the first commercial products based on it. First, there is a cost effective problem that involves the use of relatively small areas of p-Si and the safe handling of HF waste. Our group has used the specificity of DNA and the sensitivity of electrochemical detection to develop a novel, silicon compatible detection sensor for the identification of DNA. DNA hybridization has been detected voltammetrically by using ruthenium bipyridine in p-Si samples. In order to prevent the DNA probe from reacting $Ru(bpy)_3^{2+}$ with the guanosine 5'-monophosphate has been replaced from the DNA probe sequence for inosine 5'-monophosphate, which is much less reactive to oxidization. Ruthenium bipyridine showed a catalytic effect on the anodic peak current which is related to the concentration of target DNA in the hybridization reaction. The results confirmed that the DNA sensing method used here is a quick and convenient way for the specific and quantitative detection of DNA. Recently we have studied negative refraction in p-Si photonic crystals. Since negative refraction is a non-linear phenomenon, as we have shown from our simulations, the fabrication of a high sensitivity sensor that uses this effect is possible. Finally, the future will tell us whether p-Si sensing technology will reach the market giving us new and wonderful devices for medical applications or security.

6. References

Anglin E. J.; Cheng K.; Freeman W.R.; Sailor M.J. Porous silicon in drug delivery devices and materials. Advanced Drug Delivery Reviews, Vol. 60, No. 11, pp. 1266-1277.

Angelucci, R.; Poggi, A.; Critelli, C.; Dori, L.; Cavani, F.; Parisini, A.; Garulli, A.; Cardinali, G.C.; Fiorini, M. (1997). A novel gas sensor for hydrocarbons detection based on porous silicon permeated with Sn-V mixed oxides. Solid-State Device Research Conference, pp. 684 – 687.

Archer M. and Fauchet P.M. (2003). phys. Status Solidi A-Appl.Mat., Vol. 198, pp. 503.

Archer M.; Christohersen M. and Fauchet P.M. (2005). Sensors and Actuators B, Vol. 106, pp. 347-357.

Baratto C.; Faglia G.; Comini E.; Sberveglieri G.; Taroni A.; La Ferrara V.; Quercia L. and Di Francia G. (2001). A novel porous silicon sensor for detection of sub-ppm NO_2 concentrations. Sensors and Actuators B: Chemical, Vol. 77, pp. 62-66.

Baratto C.; Faglia G.; Sberveglieri G.; Gaburro Z.; Pancheri L. Oton C.J.; L. Pavesi. (2002). Multiparametric porous silicon sensors. Sensors, Vol. 2, pp. 121-126.

Ben-Chorin M.; Kux A.; and Schechter I. (1994). Appl. Phys. Lett., Vol. 64, pp. 481.

Chan S.; Li Y.; Rothberg L.J.; Miller B.L. and Fauchet P.M. (2001). Mater. Sci. Eng. C-Biomimetic Supramol.Syst., Vol. 15, pp. 2777.

Chan Selena; Horner Scott R.; Fauchet Philippe M. and Miller Benjamin L. (2001). J. Am. Chem. Soc., Vol. 123, pp. 11797-11798.

Cullis A. G. and Canham L.T. (1991). Visible light emission due to quantum size effects in highly porous crystalline silicon. Nature, Vol. 353, pp. 335-338.

Choi SH.; Cheng H.; Park SH.; Kim H.J.; Kim Y.Y and Lee K.W. (2009). A study of the gas specificity of porous silicon sensors for organic vapors. Materials science–Poland, Vol. 27, pp. 603-610

Di Francia G.; Castaldo A.; Massera E.; Nasti I.; Quercia L. and Rea I. (2005). A very sensitive porous silicon based humidity sensor. Sensors and Actuators B: Chemical Vol. 111 No. 112, pp. 135-139.

Erdem A.; Kerman K.; Meri B.; Akarca U.S. and Ozsoz M. (1999). Electroanalysis, Vol. 11, pp. 586.

Hull R. (1999). Properties of Crystalline Silicon (INSPEC, London).

Jalkanen Tero; Tuura Jaani; Mäkilä Ermei and Salonen Jarno. (2010). Electro-optical porous silicon gas sensor with enhanced selectivity. Sensors and Actuators B: Chemical Vol. 147, No. 1, pp. 100-104.

Jane A.; Dronov R.; Hodges A. and Voelcker N.H. (2009). Trends in Biotechnology - Porous silicon biosensors on the advance. Trends in Biotechnology, Vol. 27, No. 4, pp. 230-239.

Johnston D. H.; Cheng C. C.; Campbell K. J. and Thorp H. H. (1994). Inorg. Chem., Vol. 33, pp. 6388.

Johnston D. H.; Glasgow K. C. and Thorp H. H. (1995). J. Am. Chem. Soc., Vol. 117, pp. 8933.

Johnston D. H., and Thorp H. H. (1996). J. Phys. Chem., Vol. 100, pp. 13837.

Kara P.; Kerman K.; Ozkan D.; Meric B.; Erdem A.; Ozkan Z. and Ozsoz M. (2002). Electrochem. Commun., Vol. 4, pp. 705.

Kilian K. A; Böcking T. and Gooding J. J. (2009). The importance of surface chemistry in mesoporous materials: lessons from porous silicon biosensors. Chem. Commun., pp. 630-640.

Lee Mindy R. and Fauchet Philippe M. (2007). Two-dimensional silicon photonic crystal based biosensing platform for protein detection. Optics. Express, Vol. 8, pp. 4530–4535.

Lugo J.E.; Ocampo M.; Kirk A.G.; Plant D.V. and Fauchet P.M. (2007). Journal of new materials for Electrochemical Systems, Vol. 10, pp. 113-116.

Lugo J. E., de la Mora B., Doti R., Nava R., Tagueña J., del Rio A., and Faubert J., 2009, 'Multiband negative refraction in one-dimensional photonic crystals', Optics Express, Vol. 17, Issue 5, pp. 3036-3041.

Lugo J.E., Doti R. and Faubert J., 2011, 'Negative Refraction angular characterization in one dimensional photonic crystals, Plos One, to be publish.

Marraza G., Chiti G., Anichimi M., 2000, Clin. Chem., Vol. 46, 31.

Maruyama K., Motonaka J., Mishima Y., Matsuzaki Y., Nakabayashi I., Nakabayashi Y., 2001, Sens. Actuator, B-Chem., Vol. 76, 215.

McGown L, M. Joseph, J. Pitner, G. Vonk, C. Linn, 1995, Anal. Chem., Vol. 67, 663A.

Napier M. E., Loomis C. R., Sistare M. F., Kim J., Eckhardt A. E., and Thorp H. H., 1997, Bioconjugate Chem., Vol. 8, 906.

Saarinen J.J., Sipe J.E., Weiss S. and Fauchet P.M., 2005, 'Optical sensor based on resonant porous silicon structures' Quantum Electronics and Laser Science Conference, JWB38.

Schechter I., Ben-Chorin M., and Kux A., 1995,Anal. Chem., Vol. 67, 3727.

Shi L., Xiao Y., Willner I., 2004, Electrochem. Commun., Vol. 6, 1057.

Tomkeieff S.I., 1941, On the origin of the name 'quartz' .University of Durham , Newcastle upon Tyne.

Wang J., 1999, Chem. Eur. J., Vol. 5, 1681.

Yan F., Erdem A., Meric B., Kerman K., Ozsoz M., Sadik O. A., 2001, Electrochem. Commun., Vol. 3, 224.